Detection of short-lasting and ictal spike-and-wave discharges in around-the-ears EEG recordings in children with absence epilepsy

Gefferie, S.R.; Ossenblok, P.P.W.; Dietze, C.S.; Sargsyan, A.; Bourez-Swart, M.; Maagdenberg, A.M.J.M. van den; Thijs, R.D.

Epilepsy Research 204 (2024) 107385

Contents lists available at ScienceDirect

Epilepsy Research

journal homepage: www.elsevier.com/locate/epilepsyres

Detection of short-lasting and ictal spike-and-wave discharges in around-the-ears EEG recordings in children with absence epilepsy

Silvano R. Gefferie [a,b], Pauly P.W. Ossenblok [a,c], Christoph S. Dietze [a], Armen Sargsyan [d,e], Mireille Bourez-Swart [a], Arn M.J.M. van den Maagdenberg [b,f], Roland D. Thijs [a,b,g,*]

[a] Department of Clinical Neurophysiology (location Zwolle & Heemstede), Stichting Epilepsie Instellingen Nederland (SEIN), Achterweg 5, Heemstede, SW 2103, the Netherlands
[b] Department of Neurology, Leiden University Medical Centre, Albinusdreef 2, Leiden, RC 2300, the Netherlands
[c] Clinical Neuro-Science projects, De Wittenkade 283, Amsterdam, DD 1052, the Netherlands
[d] Orbeli Institute of Physiology, 22 Orbeli Bros. str 0028, Yerevan, Armenia
[e] Kaoskey Pty. Ltd., Unit 6, 3 Central Ave, Sydney, Australia
[f] Department of Human Genetics, Leiden University Medical Centre, Albinusdreef 2, Leiden, RC 2300, the Netherlands
[g] Department of Clinical & Experimental Epilepsy, UCL Queen Square Institute of Neurology, London WC1N 3BG, United Kingdom

ARTICLE INFO

Keywords:
Automatic detection
Ear electrodes
Electroencephalography
Epileptic discharge
Phase coherence

ABSTRACT

Purpose: Long-term ambulatory EEG recordings can improve the monitoring of absence epilepsy in children, but signal quality and increased review workload are a concern. We evaluated the feasibility of around-the-ears EEG arrays (cEEGrids) to capture 3-Hz short-lasting and ictal spike-and-wave discharges and assessed the performance of automated detection software in cEEGrids data. We compared patterns of bilateral synchronisation between short-lasting and ictal spike-and-wave discharges.

Methods: We recruited children with suspected generalised epilepsy undergoing routine video-EEG monitoring and performed simultaneous cEEGrids recordings. We used ASSYST software to detect short-lasting 3-Hz spike-and-wave discharges (1–3 s) and ictal spike-and-wave discharges in the cEEGrids data. We assessed data quality and sensitivity of cEEGrids for spike-and-wave discharges in routine EEG. We determined the sensitivity and false detection rate for automated spike-and-wave discharge detection in cEEGrids data. We compared bihemispheric synchrony across the onset of short-lasting and ictal spike-and-wave discharges using the mean phase coherence in the 2–4 Hz frequency band.

Results: We included nine children with absence epilepsy (median age = 11 y, range 8–15 y, nine females) and recorded 4 h and 27 min of cEEGrids data. The recordings from seven participants were suitable for quantitative analysis, containing 82 spike-and-wave discharges. The cEEGrids captured 58 % of all spike-and-wave discharges (median individual sensitivity: 100 %, range: 47–100 %). ASSYST detected 82 % of all spike-and-wave discharges (median: 100 %, range: 41–100 %) with a false detection rate of 48/h (median: 6/h, range: 0–154/h). The mean phase coherence significantly increased during short-lasting and ictal spike-and-wave discharges in the 500-ms pre-onset to 1-s post-onset interval.

Conclusions: cEEGrids are of variable quality for monitoring spike-and-wave discharges in children with absence epilepsy. ASSYST could facilitate the detection of short-lasting and ictal spike-and-wave discharges with clear periodic structures but with low specificity. A similar course of bihemispheric synchrony between short-lasting and ictal spike-and-wave discharges indicates that cortico-thalamic driving may be relevant for both types of spike-and-wave discharges.

1. Introduction

Absences manifest as a brief loss of awareness characterised by 3-Hz generalised spike-and-wave discharges (SWDs) in the EEG. By convention, a 3-s minimum duration is used to separate presumably ictal from interictal SWDs (Hirsch et al., 2022; Holmes et al., 1987). The impact of

* Correspondence to: Stichting Epilepsie Instellingen Nederland (SEIN), Hoofddorp, AM 2130, the Netherlands.
E-mail address: rthijs@sein.nl (R.D. Thijs).

https://doi.org/10.1016/j.eplepsyres.2024.107385
Received 29 March 2024; Received in revised form 23 May 2024; Accepted 29 May 2024
Available online 3 June 2024

brief non-convulsive seizures, such as absences, on cognitive development in children is well established (Nicolai et al., 2012). Converging evidence based on neuropsychological testing points towards subtle interference of brief interictal EEG abnormalities with ongoing cognitive processes such as memory, visuo-spatial and attentional functioning (Aldenkamp and Arends, 2004; Nicolai et al., 2012). For example, a fitness-to-drive test revealed that during “typical” generalised interictal epileptiform discharges (IEDs) with a median duration of 3.2 s, reaction times were prolonged by 164 ms and there was a higher likelihood of missed reactions or crashes compared to focal and “atypical” generalised IEDs (Krestel et al., 2023).

Monitoring of paroxysmal epileptiform activity in absence epilepsy usually relies on in-hospital video-EEG monitoring. While in-hospital examinations may offer a reliable evaluation of the events, these admissions are burdensome and costly, and provide a mere snapshot relative to long-term out-of-hospital recordings. Obtaining reliable seizure counts and representative indices of the effects on cognitive development are crucial to balance the possible adverse effects of anti-seizure medications on paediatric neurocognitive development (Gross-Tsur and Shalev, 2004).

Ear-EEG sensors, such as the cEEGrids (Debener et al., 2015) and the Sensor Dot, may enable long-term ambulatory recordings (Créto-t-Richert et al., 2023). They allow concealed recording of absences in adults in clinical and home environments (Swinnen et al., 2023, 2021), though in children with absence epilepsy, successful at-home recordings were made using better noticeable frontal sensors (Kjaer et al., 2017). Using artificial intelligence-based algorithms, automatic absence detection sensitivities between 79 % and 98 % (with false detection rates between 0.2/h and 4/h) have previously been established in EEG data from the Fp1-F7 derivation (Japaridze et al., 2023; Kjaer et al., 2017) and dual-channel Sensor Dot (Swinnen et al., 2023, 2021). Higher risk of artifacts probably supresses automatic detection performance in data from ambulatory compared to conventional EEG set-ups (Bernini et al., 2024), especially for brief seizures and interictal events. It, thus, remains important to assess the performance of automatic detection algorithms for these phenomena in EEG data from ambulatory equipment. ASSYST accurately detects electrographic seizures manifested by spikes and SWDs in rodent EEG data (Casillas-Espinosa et al., 2019), owing to short data processing windows and highly precise Fourier transform calculations. We hypothesised that ASSYST could detect the SWDs in human EEG as well, especially in generalised epilepsies, such as absence epilepsy. According to the International League Against Epilepsy (ILAE) classifications, SWDs occur abruptly as bilaterally synchronous generalised discharges (Hirsch et al., 2022). It has, however, been reported that bihemispheric synchrony of ictal SWDs build up gradually in a dynamic network (Gupta et al., 2011), starting preictally and leading to a fully synchronised pattern about 500 ms after ictal onset (Ossenblok et al., 2019). We additionally aimed to explore whether this phenomenon also occurs during short-lasting SWDs (<3 s).

We set out to evaluate (1) the quality and sensitivity of cEEGrids for recording short-lasting and ictal SWDs, (2) the performance of ASSYST in cEEGrids data for short-lasting and ictal SWDs compared to visual review, and (3) the peri-onset dynamics of bihemispheric synchrony during short-lasting and ictal SWDs detected in cEEGrids data.

2. Material and methods

2.1. Participants

We included children (aged 6–15 y) with a clinical suspicion of generalised epilepsy who underwent a 24-h video-EEG recording. The inclusion period covered a pilot phase, comprising the COVID pandemic and three incidental inclusions (December 2018-April 2021), and a main phase involving the remaining inclusions (March 2022-July 2023). Those not meeting the International League Against Epilepsy criteria for absence epilepsy (Hirsch et al., 2022) were excluded. The Regional Ethical Committee approved the protocol (NedMec, University Medical Centre Utrecht, The Netherlands). The children’s legal representatives provided written informed assent, as did those ≥12 years old when capable. Collected clinical variables included epilepsy syndrome classification, duration of epilepsy, currently used anti-seizure medication, MRI findings, and co-morbidities.

2.2. EEG data acquisition

Routine-EEG data were obtained using a Morpheus EEG system (Micromed S.p.A, Treviso, Italy) with 21 channels positioned according to the 10–20 system and four channels (F9, F10, P9, P10) applied according to the 10–10 system. The routine-EEG data were sampled at 256 Hz, and referenced against a supplemental electrode between Fz and Cz. We used cEEGrids arrays (TMSi B.V., Oldenzaal, Netherlands) (Debener et al., 2015), with ten channels attached around each ear (Fig. 1), for co-recording. The cEEGrids were, depending on the study phase, connected to different EEG amplifiers, including those with an online standard average reference (REFA, Mobita or SAGA; TMSi B.V., Oldenzaal, Netherlands) or with a ipsilateral mastoid reference (Smarting MOBI, mBrainTrain, Beograd, Serbia). Sampling rates were different (i.e. 500, 1000 or 2048 Hz) but as all rates well exceeded the highest frequency component in the signals prior to analysis (80 Hz), this did not affect the results. Impedances of the cEEGrids sensors were ≤30 kOhm at the start of the recording. As we lacked prior operational experience with the current systems, we wanted to ensure a stable posture of the examinee while recording (to minimize risks of EEG artifacts) and to maximise the probability of capturing SWDs. We, therefore, conducted a relatively brief co-recording that at least covered routine provocative tests such as repeated eyes closure and opening. After data acquisition, we temporally linked the cEEGrids and routine-EEG recordings.

2.3. Review of co-recorded EEG data

All co-recorded EEG data were offline bandpass filtered 0.4–80 Hz

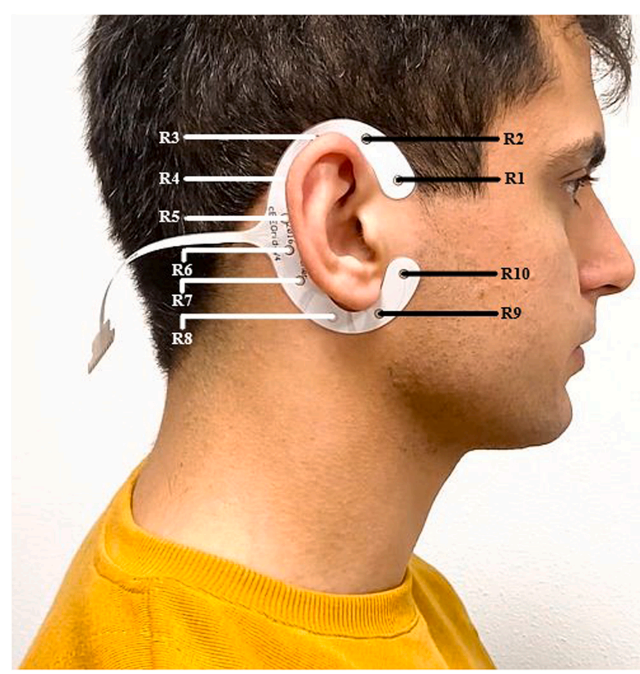

Fig. 1. Example of cEEGrids attached around the right ear. Shown are the ten cEEGrids sensors (R1–10) and their respective locations. Adapted, with permission from Twente Medical Systems International (TMSi), from: https://knowledge.tmsi.com/download-datasheet-ceegrid.

and re-referenced to the standard average. We visually appraised the quality of the cEEGrids data and excluded recordings contaminated by strong artifacts across at least half of the channels (rendering the underlying signals indiscernible) for at least 50 % of the recording. An experienced neurologist (CD) blindly annotated 3-Hz SWDs, from now on denoting a single or multiple series of spike-and-wave complexes, lasting at least 1 s in separate routine-EEG and cEEGrids recordings. SWDs lasting 3 s or longer were labelled ictal, all others as short-lasting. We defined cEEGrids recording sensitivity for SWDs as the portion of SWDs annotations in cEEGrids data compared to routine EEG.

2.4. Automated detection of SWDs in cEEGrids data

We excluded channels contaminated by artefacts more than 50 % of the recording duration and re-referenced the remaining signals to the contralateral electrode over the mastoid bone. ASSYST (Kaoskey Pty. Ltd., Sydney, Australia) has been designed to work on one channel. We, therefore, pragmatically applied the software to channel R1, which prior to each detection run visually seemed to offer the highest signal quality and SWDs amplitude. In brief, detection comprised two steps (Casilla-s-Espinosa et al., 2019). First, a time-frequency analysis was performed using a predetermined running time window (here of length 2 s with 25 % overlap) and frequency band of interest (here 9–11 Hz). We selected the 9–11 Hz band because in the first step, low-frequency signal components are removed to emphasise spikes, whose frequency spectrum in case of spike-and-wave complexes peaks in approximately this range. The spectral content was then assessed per segment using the spectral band index (SBI), being the maximum power within the chosen frequency band. Those with an SBI within automatically defined ranges were labelled candidate SWDs events. Detection of visually observed low-amplitude SWDs was facilitated by fixing the lower SBI threshold for these recordings at 1.88 μV^2, whereas for recordings with prominent artefacts, we reduced likelihood of false positive detection by setting the upper SBI threshold at 7.5 μV^2.

The second step involved the classification of candidate events into SWDs or non-SWDs. This classification was automated using a new module of ASSYST, the Running Rhytmogram Algorithm (RRA). The RRA assumes that SWDs have a regular periodic structure, while the morphology of artifacts is mostly irregular. Rhythmicity of each candidate EEG fragment is estimated based on their rhythmogram, a 2-D self-similarity matrix sensitive to subtle regularities in temporal sequences, and beat spectrum, a measure that quantifies a signals self-similarity as a function of time lag (Foote and Uchihashi, 2001; Ioannides and Sargsyan, 2012). The peaks of the beat spectrum correspond to major rhythmic components of the signal. Segments were labelled SWDs if (1) they contained a rhythmic pattern lasting $\geq$1 s, (2) the periodicity within this pattern was 2.5–4 Hz, (3) their beat spectrum contained $\geq$4 peaks, (4) the normalised amplitudes of the first three peaks exceeded 0.5, and (5) the first peak was the largest by amplitude. For cEEGrids recordings that included previously annotated short-lasting SWDs, we lowered the minimum number of beat spectrum peaks to one and fixed the minimum average value of the first three peaks at 0.1.

We compared the performance of automated SWDs detection to that of blindly annotated SWDs in the same cEEGrids data. We defined true positives (TP) as SWDs correctly identified by automated detection, false positives (FP) as EEG artefacts detected as 'SWDs', and false negatives (FN) as SWDs not identified by ASSYST. We assessed detection sensitivity [TP / (TP + FN)], and false detection rate (FDR) [FP / recording duration].

2.5. Analysis of bihemispheric synchrony in cEEGrids data

We referenced the cEEGrids data to the ipsilateral average. Next, we used custom-written scripts in MATLAB R2023b (The Mathworks Inc., Natick, MA, USA) to compute the mean phase coherence (MPC) (Mormann et al., 2000), as a measure of bihemispheric synchrony, during automatically detected SWDs. After visual screening of the SWDs, we rejected channels contaminated by artifacts and entire SWDs if no artifact-free channels remained, as these could corrupt the MPC. For the remaining SWDs and channels, the MPC in the 2–4 Hz frequency range, reflecting bilateral synchronisation of 3-Hz SWDs with a 1-Hz margin, between bilaterally-paired channels was computed from 3 s before until 3 s after onset. We used 1-s sliding windows with 90 % overlap and MPC values positioned at their centres. After averaging across channel pairs, we ran linear mixed-effects regression of MPC on time for short-lasting and ictal SWDs. Next, we performed multivariate regression of MPC on time and type of SWDs, including an interaction term for time and SWDs type. We regressed the MPC per 0.5 s segment and always included a random intercept for clustering within separate SWDs. We used *t*-tests to determine whether estimated regression effects of time and type of SWDs on the MPC were significantly different from zero. Since we repeated the regression analyses for each MPC time-frame, we selected a conservative significance threshold of $p < 0.01$.

3. Results

3.1. Participants

Fifteen children participated. Six were excluded as their syndromic diagnosis was other than absence epilepsy (n = 5) or epilepsy was not clinically confirmed (n = 1). Clinical and demographic characteristics of the remaining nine (median age = 11 y, range = 8–15 y, nine females) are presented in Table 1.

3.2. Quality and SWDs recording sensitivity of cEEGrids data

The cEEGrids recordings of two participants were excluded due to persistent (>50 % of the recording duration) major artefacts across all channels, most likely resulting from poor electrode contacts. The median duration of the remaining recordings was 21 min 42 s (range 9 min 38 s–76 min 35 s). Of the 92 short-lasting SWDs observed in the routine-EEG, 62 % were annotated in the cEEGrids data (median individual sensitivity: 100 %, range: 55–100 %), whereas of the 50 ictal SWDs seen in the routine-EEG, 50 % were annotated in the cEEGrids data (median:

Table 1
Participant demographic and clinical variables.

Participant	Sex	Age [y]	Epilepsy syndrome	Age at onset [y]	Seizure-free at inclusion	Anti-seizure medication and dose per day
1	F	8	CAE	3	No	CLB (5 mg), ESM (500 mg), VPA (750 mg),
2	F	11	CAE	3	Unknown	ESM (1000 mg)
3	F	10	CAE	5	No	VPA (1000 mg)
4	F	15	JAE	11	Yes	LVT (1000 mg)
5	F	9	CAE	6	No	LTG (250 mg)
6	F	14	JAE	10	No	ESM (500 mg)
7	F	12	CAE	9	No	LTG (300 mg), VPA (600 mg)
8	F	9	JAE	4	Unknown	LTG (75 mg)
9	F	11	CAE	7	Yes	None

CAE = childhood absence epilepsy, CLB = clobazam, ESM = ethosuximide, F = female, JAE = juvenile absence epilepsy, LTG = lamotrigine, LVT = levetiracetam, VPA = valproic acid, y = years

100 %, range: 31–100 %). Fig. 2 provides examples of a short-lasting SWDs, an ictal SWDs, and common artefacts observed in cEEGrids data. Individual SWDs annotation numbers for routine-EEG and cEEGrids recordings are provided in Table 2 and Supplementary Figure 1.

3.3. *Performance of automated SWDs detection in cEEGrids data*

We rejected a median of two cEEGrids channels (range 0–3 channels) prior to quantitative analysis. The detection sensitivity of ASSYST compared to the visual screening of SWDs in cEEGrids data amounted to 82 % (median: 100 %, range: 41–91 %) with an FDR of 48/h (median: 6/h, range: 0–154/h). The FP detections visually seemed to resemble mostly motion artifacts, with occasional sharp transients coinciding with some degree of low-frequency rhythmicity. An example of FP detection is shown in Fig. 3. Individual detection results are provided in Table 2 and Supplementary Figure 1.

3.4. *Bihemispheric synchrony during SWDs in cEEGrids data*

After artefact rejection, we selected 48 short-lasting SWDs (median duration 1.8 s, interquartile range (IQR) 1.4–2.5 s) and 17 ictal SWDs (median duration 4.5 s, IQR 3.6–9.1 s) for computing the MPC between 2.5 s before and 2.5 s after SWDs onset. Univariate regression showed significant ($p < 0.01$), positive effects of time on the MPC for three time windows, indicating significant increases. Intervals included 500-ms pre-onset until onset (short-lasting SWDs: effect = 0.13, 95 % confidence interval (CI) = [0.08 0.18]; ictal SWDs: effect = 0.14, 95 % CI = [0.05, 0.22]), onset until 500-ms post-onset (short-lasting SWDs: effect = 0.31, 95 % CI = [0.26, 0.37]; ictal SWDs: effect = 0.31, 95 % CI = [0.22, 0.41]), and 500-ms post-onset until 1-s post onset (short-lasting SWDs: effect = 0.08, 95 % CI = [0.03, 0.14]; ictal SWDs: effect = 0.25, 95 % CI = [0.19, 0.31]) (Fig. 3). The MPC was different for short-lasting compared to ictal SWDs only between 1-s and 500-ms before SWDs onset (estimated effect = 0.12, 95 % CI = [0.03, 0.20], $p < 0.01$) (Fig. 4). Though visible after approximately 0.7 s (Fig. 5), early slowing-down of MPC increase following SWDs onset for short-lasting compared to ictal SWDs did not reach significance.

4. Discussion

We found that cEEGrids capture short-lasting and ictal SWDs in children with absence epilepsy. Still, data quality and recording sensitivity for SWDs, compared to routine EEG, markedly differed between participants. Automated detection of SWDs in cEEGrids data could assist in visual review for SWDs, albeit with a high FDR. The MPC points towards prompt bihemispheric spread of ictal but also short-lasting SWDs, encouraging further studies into the subclinical, cognitive impact of short-lasting SWDs.

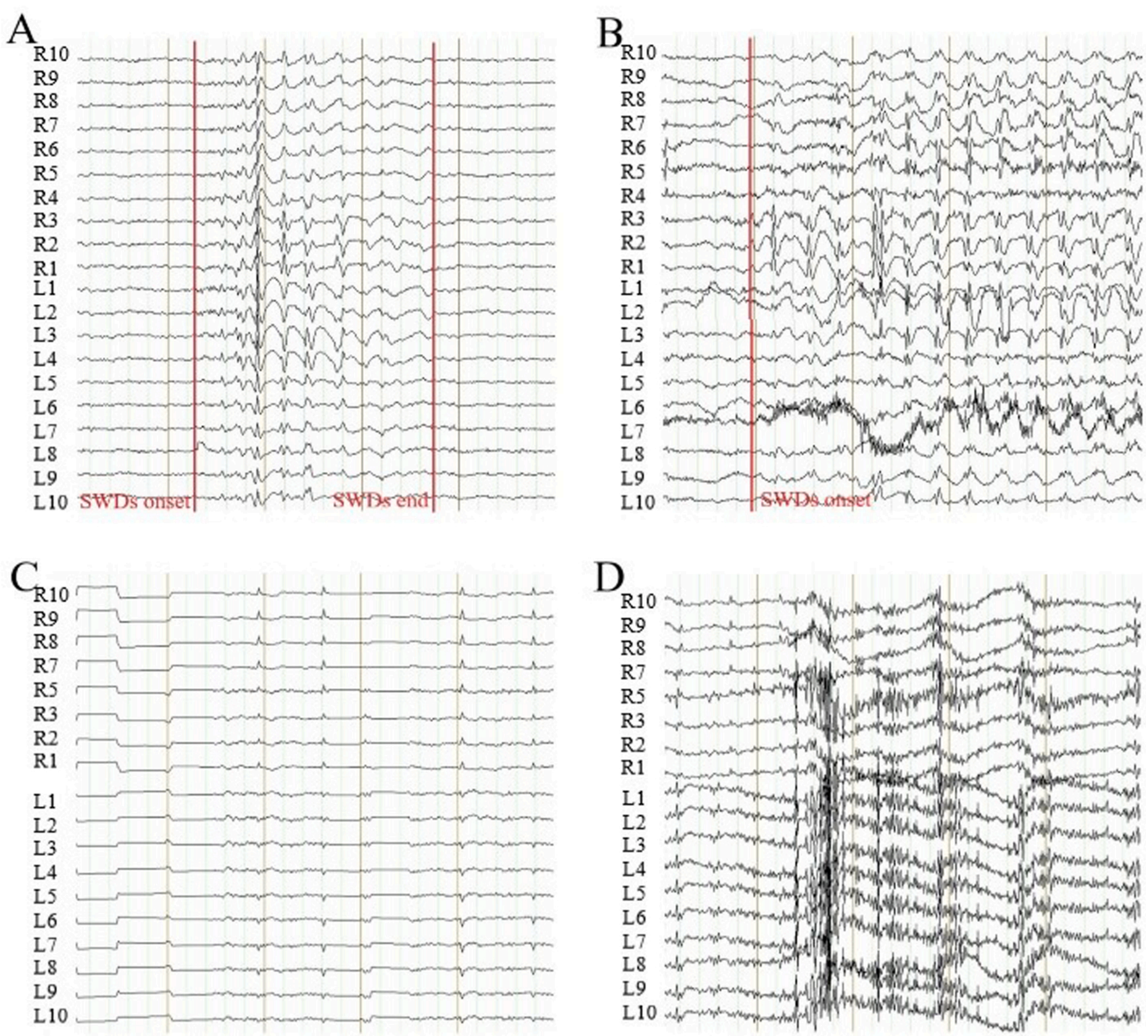

Fig. 2. Examples of cEEGrids recordings. Demonstrated are short-lasting spike-and-wave discharges (SWDs) (panel A), ictal SWDs (panel B), data loss and ECG artifacts (panel C), and muscle artifacts (panel D). Shown signals are common-average referenced and have been high-pass filtered (0.4 Hz), low-pass filtered (80 Hz), and notch filtered (50 Hz). R1–10 are right-sided electrodes, L1–10 are left-sided electrodes. Vertical scale = 100μV/cm. Time base = 5 s.

Table 2
Co-recording and automated spike-and-wave discharges detection results.

Participant	Co-recording duration	SWDs in routine-EEG [#]		SWDs in cEEGrids [#]		Correctly auto-detected SWDs [#]		FDR [/h]
		Short-lasting	Ictal	Short-lasting	Ictal	Short-lasting	Ictal	
1	9 m, 38 s	0	1	0	1	0	1	0
2	76 m, 35 s	14	3	14	3	5	2	3.1
3	50 m, 7 s	78	36	43	11	43	6	97.0
5	14 m, 2 s	0	4	0	4	0	4	154.0
6	25 m, 7 s	0	0	0	0	0	0	0
7	21 m, 42 s	0	4	0	4	0	4	5.5
8	19 m, 42 s	0	2	0	2	0	2	152.2

FDR = false detection rate, h = hour, m = minutes, s = seconds, SWDs = spike-and-wave discharges

Fig. 3. Example of a false positive (FP) spike-and-wave discharges detection. Detection was performed with ASSYST using channel R1 (label underlined in red) of cEEGrids data. Shown signals are common-average referenced and have been high-pass filtered (0.4 Hz), low-pass filtered (80 Hz), and notch-filtered (50 Hz). R1–10 are right-sided sensors, L1–10 are left-sided sensors. Vertical scale = 100μV/cm. Time base = 10 s.

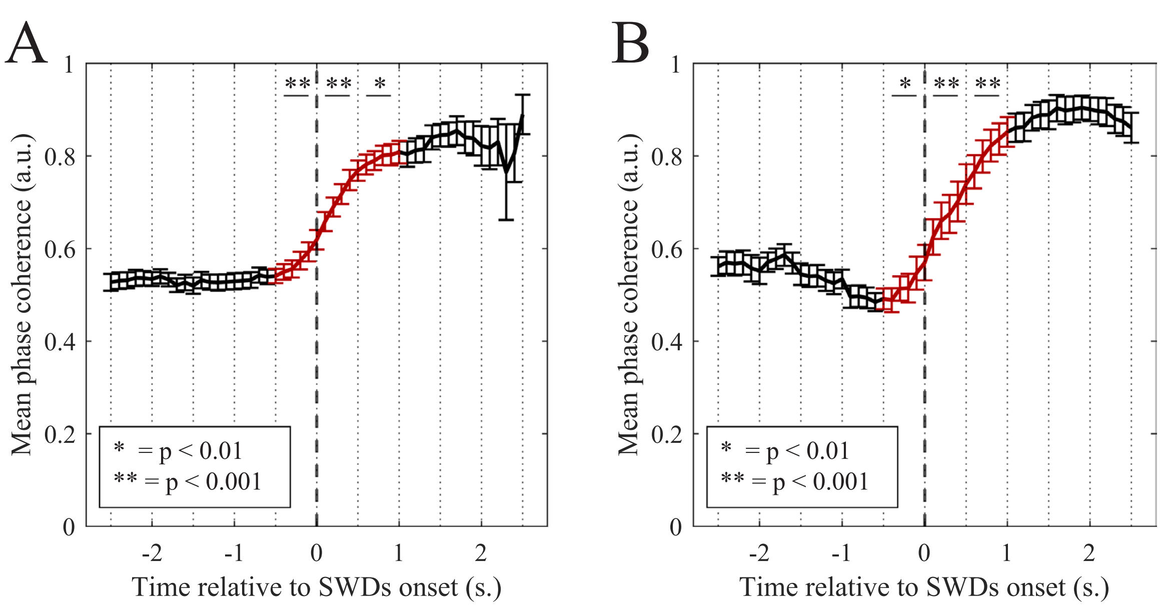

Fig. 4. Averaged mean phase coherence (MPC) between bilateral cEEGrids channel pairs. Displayed data reflect the MPC in the 2–4 Hz frequency range for short-lasting (panel A) and ictal (panel B) spike-and-wave discharges (SWDs). Subtle vertical lines demarcate separate epochs for which MPC was regressed on time. A positive effect of increasing time on the MPC was found for epochs marked red, with significance levels indicated by asterisks. Error bars represent standard error of the mean.

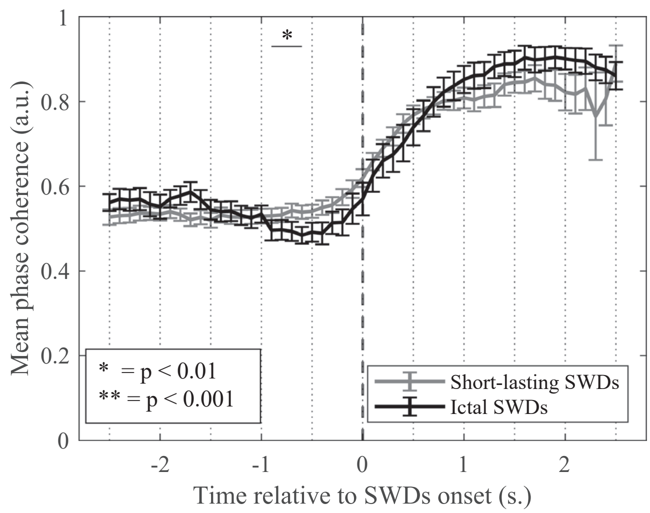

Fig. 5. Comparison of averaged mean phase coherence (MPC). Displayed data show the MPC in the 2–4 Hz frequency band for short-lasting (grey curve) and ictal (black curve) spike-and-wave discharges (SWDs). Subtle vertical lines demarcate separate epochs for which MPC was regressed on time. The epoch for which short-lasting and ictal SWDs significantly differed ($p < 0.01$) has been marked by asterisks. Error bars represent standard error of the mean.

The suboptimal data quality may be explained by an increased risk of EEG artefacts in children compared to adults (Kaiser et al., 2021). In case cEEGrids yielded acceptable data, just over half of all SWDs marked in routine-EEG data were annotated blindly in the cEEGrids data. Missed SWDs were related to one cEEGrids recording containing the most prominent ECG artefacts, which can resemble epileptiform spikes (Tatum, 2013), thus complicating visual SWDs identification. We did not restrict the visual review to entirely artefact-free episodes, allowing genuine assessment of cEEGrids sensitivity for SWDs in our clinical setting without the need for artefact-removal strategies. Further investigations may obtain more reliable recording sensitivity estimates by excluding artefact-contaminated data segments.

Sensitivities up to 98 % for automatically detecting absences using wearable EEG with frontal and frontotemporal electrodes (Japaridze et al., 2023; Kjaer et al., 2017), and behind-the-ear electrodes (Swinnen et al., 2021) have been found, exceeding automated detection performance in our study. Frontal and frontopolar electrodes may better capture maximum EEG activity during the spike components of SWDs (Ossenblok et al., 2019), which is the primary selection criterion of ASSYST. We used a standard set of detection parameters instead of machine learning for participant-wise parametric optimisation (Swinnen et al., 2021). Even though the RRA is not suited for short-lasting SWDs and SWDs with less prominent periodic features, we still applied it to all recordings for consistency with the processing approach. The RRA default criteria, however, were loosened in these cases, allowing their identification but with lower sensitivity compared to longer SWDs in other recordings and increased FDR. To allow for better comparison with visual EEG review, in future studies, ASSYST should be evaluated on different channels with a single (optimal) set of parameter values.

We found an apparent increase of bihemispheric synchrony across the onset of short-lasting and ictal SWDs. Our observation for ictal SWDs coincides with observations from animal research (Lüttjohann et al., 2014; Sysoeva et al., 2016) and human absence epilepsy studies (Gupta et al., 2011; Ossenblok et al., 2019; Youssofzadeh et al., 2018), indicating that ictal SWDs do not suddenly arise but gradually build up in a dynamic network of increasing synchronisation. Short-lasting SWDs demonstrated a similar activation pattern, though pre-onset bihemispheric synchrony was briefly lower for ictal than short-lasting SWDs. According to (Gupta et al., 2011), who performed a small-world network analysis on ictal SWDs, the dip in pre-ictal global connectivity may be specific for the interictal-to-preictal transition. Topic of future research is whether a dip in bihemispheric synchrony before the onset of SWDs has any predictive value for the occurrence of clinical symptoms. Bidirectional aberrant cortico-thalamic interactions, emerging 500 ms after ictal onset and appearing vital for the bilateral sustainment of SWDs in WAG/RIJ rats (Meeren et al., 2009, 2002), may explain the course of bihemispheric synchrony after onset of ictal SWDs. We lacked the power to detect significant post-onset differences with short-lasting SWDs due to reduction of available MPC samples with increasing time since onset. It is, however, clear from visual inspection alone that the MPC of short-lasting SWDs collapses earlier compared to ictal SWDs. Whether the initial increase of bihemispheric synchrony across the onset of short-lasting SWDs might explain the transient interference of short-lived epileptiform EEG discharges with cognition (Krestel et al., 2023; Nicolai et al., 2012) is subject to further research.

Our study was limited by its sample size, classifying it as a PHASE 1 proof-of-concept trial (Beniczky and Ryvlin, 2018). In our sample of children with absence epilepsy, we applied cEEGrids even though their dimensions were established in a pilot study in adults (Debener et al., 2015), which may have reduced the data quality. Other potential reasons for poor cEEGrids data quality encompassed artifact-prone leads and connectors, and the inability to review and correct the data quality while recording. Our choice not to reject contaminated epochs from the cEEGrids data for visual evaluation possibly caused SWDs to be partially obscured or go unnoticed. For annotated SWDs, we lacked clinical awareness indices and, thus, used the 3-s minimum duration cut-off as a surrogate marker of ictal SWD. We, differing from comparable studies (Japaridze et al., 2023; Kjaer et al., 2017; Swinnen et al., 2021), included short-lasting SWDs lasting ≥1 s in our dataset. Their clinical relevance is emphasised by evidence indicating that not only absences but also interictal SWDs are associated with impaired cognitive performances, including central information processing, visuo-motor skills and arithmetic abilities (Cheng et al., 2020; Ebus et al., 2012; Krestel et al., 2023). Our findings on bihemispheric synchrony of short-lasting and ictal SWDs onset are preliminary and restricted to cEEGrids data, though similar observations were made for absences in MEG and routine scalp-EEG studies (Ossenblok et al., 2019; Ponten et al., 2009). Further studies involving sensitive time-resolved awareness metrics are needed to validate bihemispheric synchrony as an EEG marker of subtle cognitive impairment during short-lasting SWDs.

Funding

This work was supported by Health-Holland, Top Sector Life Sciences & Health, Netherlands Organization for Health Research and Development (ZonMW) [Brain@Home, Project number: 114025101] (to AMJMvdM and RDT), and the Christelijke Vereniging voor de Verpleging van Lijders aan Epilepsie (to RDT). The funding sources did not have any involvement in the study design; collection, analysis and interpretation of data; writing of the report; and decision to submit the article for publication.

Author contributions

Silvano R. Gefferie, Pauly P.W. Ossenblok, Christoph S. Dietze, Mireille Bourez-Swart, and Arn M.J.M. van den Maagdenberg have no relevant disclosures. Armen Sargsyan is a researcher at Kaoskey Pty. Ltd. Roland D. Thijs reports lecture and consultancy fees from Medtronic, UCB, Theravarance, Zogenix, Novartis, and Arvelle, and grants from EpilepsieNL, Medtronic, Michael J Fox Foundation, NewLife Wearables, and The Netherlands Organisation for Health Research and Development.

CRediT authorship contribution statement

Mireille Bourez-Swart: Writing – review & editing, Supervision, Resources, Conceptualization. **Armen Sargsyan:** Writing – review & editing, Software, Methodology. **Roland D. Thijs:** Writing – review & editing, Project administration, Methodology, Funding acquisition, Conceptualization. **Arn M.J.M. van den Maagdenberg:** Writing – review & editing, Project administration, Funding acquisition. **Silvano R. Gefferie:** Writing – review & editing, Writing – original draft, Visualization, Software, Project administration, Methodology, Investigation, Formal analysis, Data curation, Conceptualization. **Christoph S. Dietze:** Writing – review & editing, Methodology, Data curation. **Pauly P.W. Ossenblok:** Writing – review & editing, Validation, Methodology, Conceptualization.

Data Availability

The data supporting the findings of this study are available upon reasonable request.

Acknowledgements

The authors would like to thank all participants for participating in this study. We would also like to extent our gratitude to Miranda Meijberg and Aniek Grimme for assistance with the cEEGrids recordings.

Appendix A. Supporting information

Supplementary data associated with this article can be found in the online version at doi:10.1016/j.eplepsyres.2024.107385.

References

Aldenkamp, A., Arends, J., 2004. The relative influence of epileptic EEG discharges, short nonconvulsive seizures, and type of epilepsy on cognitive function. Epilepsia 45, 54–63. https://doi.org/10.1111/j.0013-9580.2004.33403.x.

Beniczky, S., Ryvlin, P., 2018. Standards for testing and clinical validation of seizure detection devices. Epilepsia 59 (Suppl 1), 9–13. https://doi.org/10.1111/epi.14049.

Bernini, A., Dan, J., Ryvlin, P., 2024. Ambulatory seizure detection. Curr. Opin. Neurol. 37, 99–104. https://doi.org/10.1097/WCO.0000000000001248.

Casillas-Espinosa, P.M., Sargsyan, A., Melkonian, D., O'Brien, T.J., 2019. A universal automated tool for reliable detection of seizures in rodent models of acquired and genetic epilepsy. Epilepsia 60, 783–791. https://doi.org/10.1111/epi.14691.

Cheng, D., Yan, X., Xu, K., Zhou, X., Chen, Q., 2020. The effect of interictal epileptiform discharges on cognitive and academic performance in children with idiopathic epilepsy. BMC Neurol. 20, 233. https://doi.org/10.1186/s12883-020-01807-z.

Crétot-Richert, G., De Vos, M., Debener, S., Bleichner, M.G., Voix, J., 2023. Assessing focus through ear-EEG: a comparative study between conventional cap EEG and mobile in- and around-the-ear EEG systems. Front. Neurosci. 17, 895094 https://doi.org/10.3389/fnins.2023.895094.

Debener, S., Emkes, R., De Vos, M., Bleichner, M., 2015. Unobtrusive ambulatory EEG using a smartphone and flexible printed electrodes around the ear. Sci. Rep. 5, 16743 https://doi.org/10.1038/srep16743.

Ebus, S., Arends, J., Hendriksen, J., van der Horst, E., de la Parra, N., Hendriksen, R., Santegoeds, E., Boon, P., Aldenkamp, B., 2012. Cognitive effects of interictal epileptiform discharges in children. Eur. J. Paediatr. Neurol. EJPN . J. Eur. Paediatr. Neurol. Soc. 16, 697–706. https://doi.org/10.1016/j.ejpn.2012.05.010.

Foote, J., Uchihashi, S., 2001. The beat spectrum: a new approach to rhythm analysis. : IEEE Int. Conf. Multimed. Expo. 2001. ICME 2001. 881–884. https://doi.org/10.1109/ICME.2001.1237863.

Gross-Tsur, V., Shalev, R.S., 2004. Reversible language regression as an adverse effect of topiramate treatment in children. Neurology 62, 299–300. https://doi.org/10.1212/01.wnl.0000103285.85821.b3.

Gupta, D., Ossenblok, P., van Luijtelaar, G., 2011. Space-time network connectivity and cortical activations preceding spike wave discharges in human absence epilepsy: a MEG study. Med. Biol. Eng. Comput. 49, 555–565. https://doi.org/10.1007/s11517-011-0778-3.

Hirsch, E., French, J., Scheffer, I.E., Bogacz, A., Alsaadi, T., Sperling, M.R., Abdulla, F., Zuberi, S.M., Trinka, E., Specchio, N., Somerville, E., Samia, P., Riney, K., Nabbout, R., Jain, S., Wilmshurst, J.M., Auvin, S., Wiebe, S., Perucca, E., Moshé, S.L., Tinuper, P., Wirrell, E.C., 2022. ILAE definition of the idiopathic generalized epilepsy syndromes: position statement by the ILAE task force on nosology and definitions. Epilepsia 63, 1475–1499. https://doi.org/10.1111/epi.17236.

Holmes, G.L., McKeever, M., Adamson, M., 1987. Absence seizures in children: clinical and electroencephalographic features. Ann. Neurol. 21, 268–273. https://doi.org/10.1002/ana.410210308.

Ioannides, A.A., Sargsyan, A., 2012. Rhythmogram-based analysis for continuous electrographic data of the human brain. IEEE Trans. Inf. Technol. Biomed. a Publ. IEEE Eng. Med. Biol. Soc. 16, 205–211. https://doi.org/10.1109/TITB.2011.2170217.

Japaridze, G., Loeckx, D., Buckinx, T., Armand Larsen, S., Proost, R., Jansen, K., MacMullin, P., Paiva, N., Kasradze, S., Rotenberg, A., Lagae, L., Beniczky, S., 2023. Automated detection of absence seizures using a wearable electroencephalographic device: a phase 3 validation study and feasibility of automated behavioral testing. Suppl 4, S40–S46 Epilepsia 64. https://doi.org/10.1111/epi.17200.

Kaiser, A., Aggensteiner, P.-M., Holtmann, M., Fallgatter, A., Romanos, M., Abenova, K., Alm, B., Becker, K., Döpfner, M., Ethofer, T., Freitag, C.M., Geissler, J., Hebebrand, J., Huss, M., Jans, T., Jendreizik, L.T., Ketter, J., Legenbauer, T., Philipsen, A., Poustka, L., Renner, T., Retz, W., Rösler, M., Thome, J., Uebel-von Sandersleben, H., von Wirth, E., Zinnow, T., Hohmann, S., Millenet, S., Holz, N.E., Banaschewski, T., Brandeis, D., ESCAlife-Consortium, O.B.O.T., 2021. EEG Data Quality: Determinants and Impact in a Multicenter Study of Children, Adolescents, and Adults with Attention-Deficit/Hyperactivity Disorder (ADHD). Brain Sci. 11. https://doi.org/10.3390/brainsci11020214.

Kjaer, T.W., Sorensen, H.B.D., Groenborg, S., Pedersen, C.R., Duun-Henriksen, J., 2017. Detection of paroxysms in long-term, single-channel EEG-monitoring of patients with typical absence seizures. IEEE J. Transl. Eng. Heal. Med. 5, 2000108. https://doi.org/10.1109/JTEHM.2017.2649491.

Krestel, H., Schreier, D.R., Sakiri, E., von Allmen, A., Abukhadra, Y., Nirkko, A., Steinlin, M., Rosenow, F., Markhus, R., Schneider, G., Jagella, C., Mathis, J., Blumenfeld, H., 2023. Predictive power of interictal epileptiform discharges in fitness-to-drive evaluation. Neurology 101, e866–e878. https://doi.org/10.1212/WNL.0000000000207531.

Lüttjohann, A., Schoffelen, J.-M., van Luijtelaar, G., 2014. Termination of ongoing spike-wave discharges investigated by cortico-thalamic network analyses. Neurobiol. Dis. 70, 127–137. https://doi.org/10.1016/j.nbd.2014.06.007.

Meeren, H.K.M., Pijn, J.P.M., Van Luijtelaar, E.L.J.M., Coenen, A.M.L., da Silva, F.H., 2002. Cortical Focus Drives Widespread Corticothalamic Networks during Spontaneous Absence Seizures in Rats. J. Neurosci. 22, 1480–1495. https://doi.org/10.1523/JNEUROSCI.22-04-01480.2002.

Meeren, H.K.M., Veening, J.G., Möderscheim, T.A.E., Coenen, A.M.L., van Luijtelaar, G., 2009. Thalamic lesions in a genetic rat model of absence epilepsy: dissociation between spike-wave discharges and sleep spindles. Exp. Neurol. 217, 25–37. https://doi.org/10.1016/j.expneurol.2009.01.009.

Mormann, F., Lehnertz, K., David, P., E. Elger, C., 2000. Mean phase coherence as a measure for phase synchronization and its application to the EEG of epilepsy patients. Phys. D. Nonlinear Phenom. 144, 358–369. https://doi.org/10.1016/S0167-2789(00)00087-7.

Nicolai, J., Ebus, S., Biemans, D.P.L.J.J.G., Arends, J., Hendriksen, J., Vles, J.S.H., Aldenkamp, A.P., 2012. The cognitive effects of interictal epileptiform EEG discharges and short nonconvulsive epileptic seizures. Epilepsia 53, 1051–1059. https://doi.org/10.1111/j.1528-1167.2012.03491.x.

Ossenblok, P., van Houdt, P., Colon, A., Stroink, H., van Luijtelaar, G., 2019. A network approach to investigate the bi-hemispheric synchrony in absence epilepsy. Clin. Neurophysiol. Off. J. Int. Fed. Clin. Neurophysiol. 130, 1611–1619. https://doi.org/10.1016/j.clinph.2019.05.034.

Ponten, S.C., Douw, L., Bartolomei, F., Reijneveld, J.C., Stam, C.J., 2009. Indications for network regularization during absence seizures: weighted and unweighted graph theoretical analyses. Exp. Neurol. 217, 197–204. https://doi.org/10.1016/j.expneurol.2009.02.001.

Swinnen, L., Chatzichristos, C., Jansen, K., Lagae, L., Depondt, C., Seynaeve, L., Vancaester, E., Van Dycke, A., Macea, J., Vandecasteele, K., Broux, V., De Vos, M., Van Paesschen, W., 2021. Accurate detection of typical absence seizures in adults and children using a two-channel electroencephalographic wearable behind the ears. Epilepsia 62, 2741–2752. https://doi.org/10.1111/epi.17061.

Swinnen, L., Chatzichristos, C., Bhagubai, M., Broux, V., Zabler, N., Dümpelmann, M., Schulze-Bonhage, A., De Vos, M., Van Paesschen, W., 2023. Home recording of 3-Hz spike-wave discharges in adults with absence epilepsy using the wearable Sensor Dot. Epilepsia. https://doi.org/10.1111/epi.17839.

Sysoeva, M.V., Lüttjohann, A., van Luijtelaar, G., Sysoev, I.V., 2016. Dynamics of directional coupling underlying spike-wave discharges. Neuroscience 314, 75–89. https://doi.org/10.1016/j.neuroscience.2015.11.044.

Tatum, W.O., 2013. Artifact-related epilepsy. Neurology 80, S12–S25. https://doi.org/10.1212/WNL.0b013e3182797325.

Youssofzadeh, V., Agler, W., Tenney, J.R., Kadis, D.S., 2018. Whole-brain MEG connectivity-based analyses reveals critical hubs in childhood absence epilepsy. Epilepsy Res. 145, 102–109. https://doi.org/10.1016/j.eplepsyres.2018.06.001.